ARTICLE

doi:10.1038/nature12988

In vivo discovery of immunotherapy targets in the tumour microenvironment

Penghui Zhou[1]*, Donald R. Shaffer[1]*†, Diana A. Alvarez Arias[1], Yukoh Nakazaki[1], Wouter Pos[1], Alexis J. Torres[2], Viviana Cremasco[1], Stephanie K. Dougan[3], Glenn S. Cowley[4], Kutlu Elpek[1]†, Jennifer Brogdon[5], John Lamb[6], Shannon J. Turley[1], Hidde L. Ploegh[3], David E. Root[4], J. Christopher Love[2], Glenn Dranoff[1], Nir Hacohen[4], Harvey Cantor[1] & Kai W. Wucherpfennig[1]

Recent clinical trials showed that targeting of inhibitory receptors on T cells induces durable responses in a subset of cancer patients, despite advanced disease. However, the regulatory switches controlling T-cell function in immunosuppressive tumours are not well understood. Here we show that such inhibitory mechanisms can be systematically discovered in the tumour microenvironment. We devised an *in vivo* pooled short hairpin RNA (shRNA) screen in which shRNAs targeting negative regulators became highly enriched in murine tumours by releasing a block on T-cell proliferation upon tumour antigen recognition. Such shRNAs were identified by deep sequencing of the shRNA cassette from T cells infiltrating tumour or control tissues. One of the target genes was *Ppp2r2d*, a regulatory subunit of the PP2A phosphatase family. In tumours, *Ppp2r2d* knockdown inhibited T-cell apoptosis and enhanced T-cell proliferation as well as cytokine production. Key regulators of immune function can therefore be discovered in relevant tissue microenvironments.

Recent work has shown that cytotoxic T cells have a central role in immune-mediated control of cancer[1–7]. T cells are able to specifically detect and eliminate cancer cells following T-cell receptor (TCR)-mediated recognition of tumour-derived peptides bound to MHC proteins[8]. A series of studies have convincingly demonstrated that the extent of tumour infiltration by cytotoxic T cells is a critical factor determining the natural progression of diverse types of cancers[1–4,9–11]. A landmark study showed that the type, density and location of cytotoxic T cells within tumours enabled better prediction of patient survival than histopathological methods used for staging of cancers[1]. Strong infiltration of both the tumour centre and the invasive tumour margin by cytotoxic T cells (which express the CD8 surface marker) was shown to correlate with a favourable prognosis, regardless of the local extent of tumour invasion and spread to local lymph nodes. Conversely, weak *in situ* expansion of CD8 T cells correlated with a poor prognosis even in patients with minimal tumour invasion[1]. However, in the majority of patients this natural defence mechanism is severely blunted by immunosuppressive cell populations recruited to the tumour microenvironment, including regulatory T cells, immature myeloid cell populations and tumour-associated macrophages[4,12–14]. Highly complex interactions among a variety of different cell types in the tumour microenvironment—including tumour cells, immune cells and stromal cells—therefore contribute to clinical outcome.

The critical role of T cells in immune-mediated control of cancers is further underscored by therapeutic benefit following administration of monoclonal antibodies targeting inhibitory receptors on T cells, CTLA-4 and PD-1[15–18]. Clinical benefit is enhanced by co-administration of antibodies targeting CTLA-4 and PD-1[19,20]. Particularly notable is the finding that such antibodies can induce durable responses in a subset of patients with advanced disease. However, many of the regulatory pathways in T cells that result in loss of function within immunosuppressive tumour microenvironments remain unknown.

Immune cells perform complex surveillance functions throughout the body and interact with many different types of cells in distinct tissue microenvironments. Therapeutic targets for modulating immune responses are typically identified *in vitro* and tested in animal models at a late stage of the process. We postulated that the complex interactions of immune cells within tissues, many of which do not occur *in vitro*, offer untapped opportunities for therapeutic intervention. Here we have addressed the challenge of how targets for immune modulation can be systematically discovered *in vivo*.

Design of *in vivo* discovery approach

Pooled shRNA libraries have been shown to be powerful discovery tools[21–23]. We reasoned that shRNAs capable of restoring CD8 T-cell function can be systematically discovered *in vivo* by taking advantage of the extensive proliferative capacity of T cells following triggering of the TCR by a tumour-associated antigen. When introduced into T cells, only a small subset of shRNAs from a pool will restore T-cell proliferation, resulting in their enrichment within tumours. Over-representation of active shRNAs within a pool can be quantified by deep sequencing of the shRNA cassette from tumours and secondary lymphoid organs (Fig. 1a).

We chose to study B16 melanoma, an aggressive tumour that is difficult to treat[24]. Melanoma cells expressed the surrogate tumour antigen ovalbumin (Ova), which is recognized by CD8 T cells from OT-I T-cell receptor transgenic mice[25,26]. Initial experiments showed that such a screen could also be performed with pmel-1 T cells that recognize gp100, an endogenous melanoma antigen[27], but the signal/noise ratio was lower for pmel-1 T cells owing to smaller T-cell populations in tumours. Naive T cells are difficult to infect with lentiviral vectors, and we therefore pretreated T cells for two days with the homeostatic cytokines IL-7 and IL-15 before spin infection with shRNA pools in a lentiviral vector. Successful transduction was monitored by surface expression of the Thy1.1 reporter (Extended Data Fig. 1a). T cells were injected into B6 mice bearing day 14 B16-Ova tumours. Seven days later, T cells were purified from tumours and secondary lymphoid

[1]Dana-Farber Cancer Institute, Boston, Massachusetts 02115, USA. [2]David H. Koch Institute for Integrative Cancer Research, Massachusetts Institute of Technology, Cambridge, Massachusetts 02142, USA. [3]Whitehead Institute, Massachusetts Institute of Technology, Cambridge, Massachusetts 02142, USA. [4]Broad Institute of MIT and Harvard, Cambridge, Massachusetts 02142, USA. [5]Novartis Institutes for Biomedical Research, Cambridge, Massachusetts 02139, USA. [6]Genomics Institute of the Novartis Research Foundation, San Diego, California 92121, USA. †Present address: Jounce Therapeutics, Cambridge, Massachusetts 02138, USA.
*These authors contributed equally to this work.

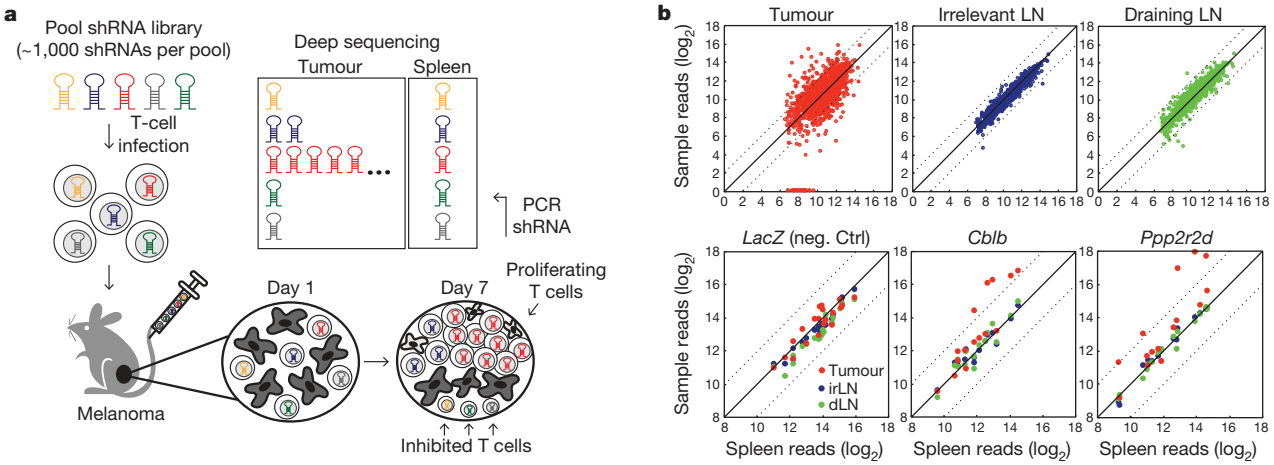

Figure 1 | *In vivo* RNAi discovery of immunotherapy targets. **a**, *In vivo* discovery approach for negative regulators of T-cell function in tumours. T cells infected with shRNA libraries were injected into tumour-bearing mice; shRNAs that enabled T-cell accumulation in tumours were identified by deep sequencing of the shRNA cassette from purified T cells. **b**, Deep sequencing data: shRNA sequence reads from tumours, irrelevant (irLN) and draining lymph nodes (dLN) versus spleen. Upper row, sequence reads for all genes in a pool; lower row, individual genes (*LacZ*, negative control). Dashed lines indicate a deviation by $\log_2$ from diagonal.

organs (spleen, tumour-draining and irrelevant lymph nodes) for isolation of genomic DNA, followed by PCR amplification of the shRNA cassette (Extended Data Fig. 1b). The representation of shRNAs was then quantified in different tissues by Illumina sequencing.

In vivo shRNA pool screens

Two large screens were performed, with the first focusing on genes overexpressed in dysfunctional T cells (T-cell anergy or exhaustion; 255 genes, 1,275 shRNAs divided into two pools), and the second on kinases/phosphatases (1,307 genes, 6,535 shRNAs divided into seven pools) (Table 1a). In these primary screens, each gene was represented by approximately five shRNAs (it is common that only one or two of such shRNAs have sufficient activity in pooled screens). We observed multiple distinct *in vivo* phenotypes. For certain genes, shRNAs were over-represented in all tested tissues compared to the starting T-cell population (for example, SHP-1), indicative of enhanced proliferation independent of TCR recognition of a tumour antigen. For other genes, there was a selective loss of shRNAs within tumours (for example, ZAP-70, a critical kinase in the T-cell activation pathway). We focused our analysis on genes whose shRNAs showed substantial over-representation in tumour but not spleen, a secondary lymphoid organ. Substantial T-cell accumulation in tumours was observed for a number of shRNAs, despite the immunosuppressive environment. For secondary screens, we created focused pools in which each candidate gene was represented by approximately 15 shRNAs. Primary data from this analysis are shown for three genes in Fig. 1b: *LacZ* (negative control), *Cblb* (an E3 ubiquitin ligase that induces T-cell receptor internalization)[28] and *Ppp2r2d* (not previously studied in T cells). For both *Ppp2r2d* and *Cblb*, five shRNAs were substantially increased in tumours (red) compared to spleen, whereas no enrichment was observed for *LacZ* shRNAs. Overall, 43 genes met the following criteria: ≥ fourfold enrichment for three or more shRNAs in tumours compared to spleen (Table 1a and Extended Data Fig. 1c, d). The set included gene products previously identified as inhibitors of T-cell receptor signalling (including *Cblb*, *Dgka*, *Dgkz*, *Ptpn2*), as well as other well-known inhibitors of T-cell function (for example, *Smad2*, *Socs1*, *Socs3*, *Egr2*), validating our approach (Table 1b and Extended Data Table 1)[29–31].

Target validation

We next confirmed at a cellular level that these shRNAs induce T-cell accumulation in tumours. OT-I T cells were infected with lentiviral vectors driving expression of a single shRNA and a reporter protein (Thy1.1 or one of four different fluorescent proteins), and after seven days the frequency of shRNA-transduced T cells was quantified in tumours, spleens and lymph nodes by flow cytometry. When the control *LacZ* shRNA was expressed in CD8 T cells, the frequency of shRNA-expressing CD8 T cells was lower in tumours compared to spleen (~twofold). In contrast, experimental shRNAs induced accumulation

Table 1 | Summary of primary and secondary shRNA screens

a		T-cell dysfunction	Kinase/phosphatase	shRNA enrichment in tumour
First screen	Genes	255	1,307	4–10-fold: 123
	shRNAs	1,275	6,535	10–20-fold: 17
	Candidate genes	32	82	>20-fold: 1
Second screen	Genes	32	43	4–10-fold: 191
	shRNAs	480	645	10–20-fold: 27
	Candidate genes	17	26	>20-fold: 1

b	Function	Genes
	Inhibition of TCR signalling	*Cblb*, *Dgka*, *Dgkz*, *Fyn*, *Inpp5b*, *Ppp3cc*, *Ptpn2*, *Stk17b*, *Tnk1*
	Phosphoinositol metabolism	*Dgka*, *Dgkz*, *Impk*, *Inpp5b*, *Sbf1*
	Inhibitory cytokine signalling pathways	*Smad2*, *Socs1*, *Socs3*
	AMP signalling, Inhibition of mTOR	*Entpd1*, *Prkab2*, *Nuak*
	Cell cycle	*Cdkn2a*, *Pkd1*, *Ppp2r2d*
	Actin and microtubules	*Arhgap5*, *Mast2*, *Rock1*
	Potential nuclear functions	*Blvrb*, *Egr2*, *Impk*, *Jun*, *Ppm1g*
	Role in cancer cells	*Alk*, *Arhgap5*, *Eif2ak3*, *Hipk1*, *Met*, *Nuak*, *Pdzk1ip1*, *Rock1*, *Yes1*

a, T-cell dysfunction and kinase/phosphatase screens. Listed are numbers of genes, shRNAs in each gene set and identified candidate genes. Genes were considered positive in secondary screens when ≥ 3 shRNAs showed ≥ fourfold enrichment in tumour relative to spleen. **b**, Functional classification of candidate genes from secondary screens.

of CD8 T cells in tumours but not in the spleen (Fig. 2a and Extended Data Fig. 2a). T-cell accumulation in tumours was more than tenfold relative to spleen for seven of these genes. The strongest phenotype was observed with shRNAs targeting *Ppp2r2d*, a regulatory subunit of the family of PP2A phosphatases[32]. A *Ppp2r2d* shRNA not only induced accumulation of OT-I CD8 T cells, but also CD4 T cells (from TRP-1 TCR transgenic mice)[33], with T-cell numbers in tumours being significantly higher when *Ppp2r2d* rather than *LacZ* shRNA was expressed (36.3-fold for CD8; 16.2-fold for CD4 T cells) (Fig. 2b). CD8 T-cell accumulation correlated with the degree of *Ppp2r2d* knockdown, and two *Ppp2r2d* shRNAs with the highest *in vivo* activity induced the lowest levels of *Ppp2r2d* messenger RNA (Extended Data Fig. 2b). *Ppp2r2d* knockdown was also confirmed at the protein level using a quantitative mass spectrometry approach (Fig. 2e). *Ppp2r2d* shRNA activity was specific because the phenotype was reversed when a *Ppp2r2d* complementary DNA (with wild-type protein sequence, but mutated DNA sequence at the shRNA binding site) was co-introduced with the *Ppp2r2d* shRNA (Fig. 2c and Extended Data Fig. 3). Furthermore, OT-I CD8 T cells overexpressed *Ppp2r2d* in tumours compared to spleen (in the absence of any shRNA expression), indicating that it is an intrinsic component of the signalling network inhibiting T-cell function in tumours (Fig. 2d). Microarray analysis of tumour-infiltrating T cells expressing different shRNAs showed that each shRNA induced a largely distinct set of gene expression changes, indicating that improved T-cell function in tumours can be mediated through a number of different intracellular pathways (Extended Data Fig. 4).

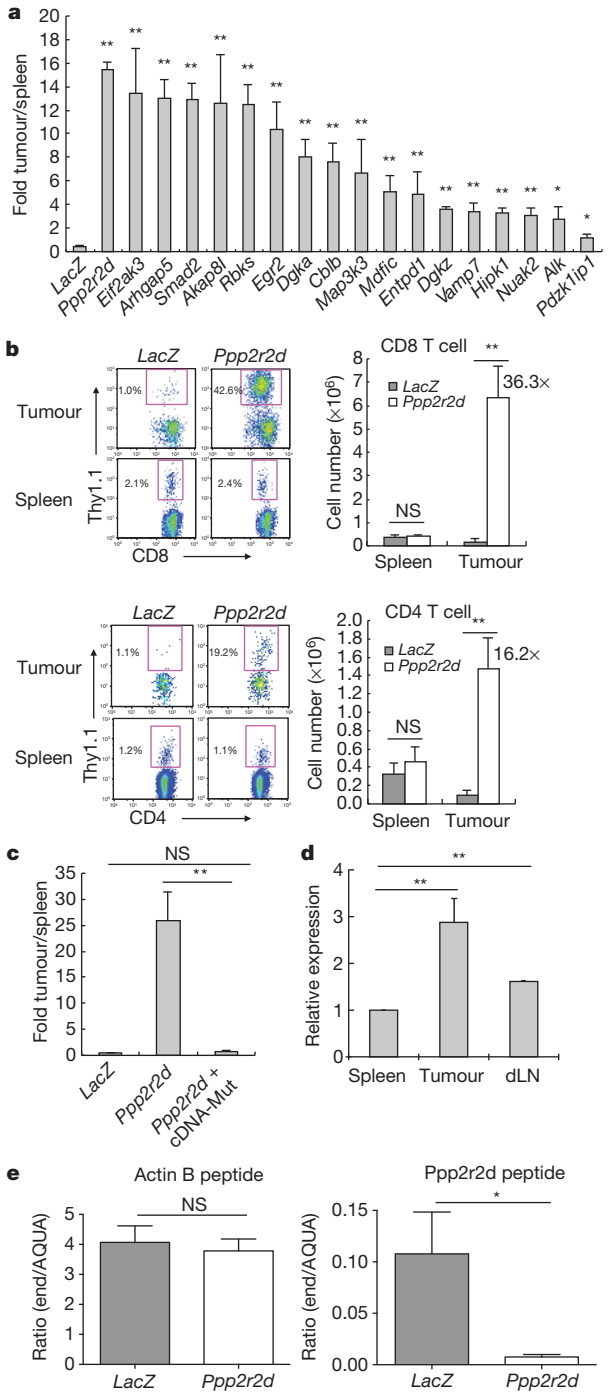

Figure 2 | shRNA-driven accumulation of T cells in B16 melanoma. **a**, CD8 (OT-I) T-cell enrichment in tumours relative to spleen ($n = 3$). **b**, Enrichment of *Ppp2r2d*-silenced CD8 (OT-I) or CD4 (TRP1) T cells (Thy1.1$^+$ cells) in tumour versus spleen. **c**, Reversal of shRNA-induced phenotype by *Ppp2r2d* cDNA with mutated shRNA binding site. NS, not significant. **d**, Quantitative PCR for *Ppp2r2d* mRNA in tumour-infiltrating OT-I T cells (day 7). **e**, Ppp2r2d protein quantification by mass spectrometry with labelled synthetic peptides (AQUA, ratio of endogenous to AQUA peptides). Representative data from two independent experiments (**a**–**d**); Two-sided student's *t*-test, $*P \leq 0.05$, $**P \leq 0.01$; mean ± s.d.

Cellular mechanisms for *Ppp2r2d*

We next examined the cellular mechanisms driving T-cell accumulation by a *Ppp2r2d* shRNA in tumours, specifically T-cell infiltration, proliferation and apoptosis. T-cell infiltration into tumours was assessed by transfer of OT-I CD8 T cells labelled with a cytosolic dye (carboxyfluorescein succinimidyl ester, CFSE). No differences were observed in the frequency of *Ppp2r2d* or *LacZ* shRNA-transduced CD8 T cells in tumours on day 1, indicating no substantial effect on T-cell infiltration (Fig. 3a). However, analysis of later time points (days 3–7) demonstrated a higher degree of proliferation (based on CFSE dilution) by *Ppp2r2d* compared to *LacZ* shRNA-transduced T cells (Fig. 3b and Extended Data Fig. 5a). The action of *Ppp2r2d* was downstream of T-cell receptor activation because T-cell proliferation was enhanced in tumours and to a lesser extent in tumour-draining lymph nodes (Extended Data Fig. 5a). In contrast, no proliferation was observed in irrelevant lymph nodes or the spleen where the relevant antigen was not presented to T cells (data not shown). Substantial T-cell proliferation was even observed for *LacZ* shRNA-transduced T cells (complete dilution of CFSE dye by day 7), despite the presence of small numbers of such cells in tumours. This indicated that *LacZ* shRNA-transduced T cells were lost by apoptosis. Indeed, a larger percentage of tumour-infiltrating T cells were labelled with an antibody specific for active caspase 3 when the *LacZ* control shRNA (rather than *Ppp2r2d* shRNA) was expressed (Fig. 3c and Extended Data Fig. 5b). Furthermore, co-culture of CD8 T cells with B16-Ova tumour cells showed that the majority of *LacZ* shRNA-expressing T cells became apoptotic (65.7%), whereas most *Ppp2r2d* shRNA-transduced T cells were viable (89.5%, Fig. 3d).

These results indicated the possibility that *Ppp2r2d* shRNA-transduced CD8 T cells may be able to proliferate and survive even when they recognize their antigen directly presented by B16-Ova tumour cells. This idea was tested by implantation of tumour cells into *B2m*$^{-/-}$ mice which are deficient in expression of MHC class I proteins[34]. In such mice, only tumour cells of the host, but not professional antigen-presenting cells, could present tumour antigens to T cells. Indeed, *Ppp2r2d* shRNA-transduced OT-I CD8 T cells showed massive accumulation within B16-Ova tumours in *B2m*$^{-/-}$ mice (Fig. 3e) whereas very small numbers of T cells were present in contralateral B16 tumours that lacked expression of the Ova antigen. *Ppp2r2d*-silenced T cells could therefore effectively proliferate and survive in response to tumour cells, despite a lack of suitable co-stimulatory signals and an inhibitory microenvironment.

Ex vivo analysis of tumour-infiltrating T cells at a single-cell level using a nanowell device[35,36] also demonstrated that *Ppp2r2d* silencing increased cytokine production by T cells (Fig. 4a–c). T cells were activated

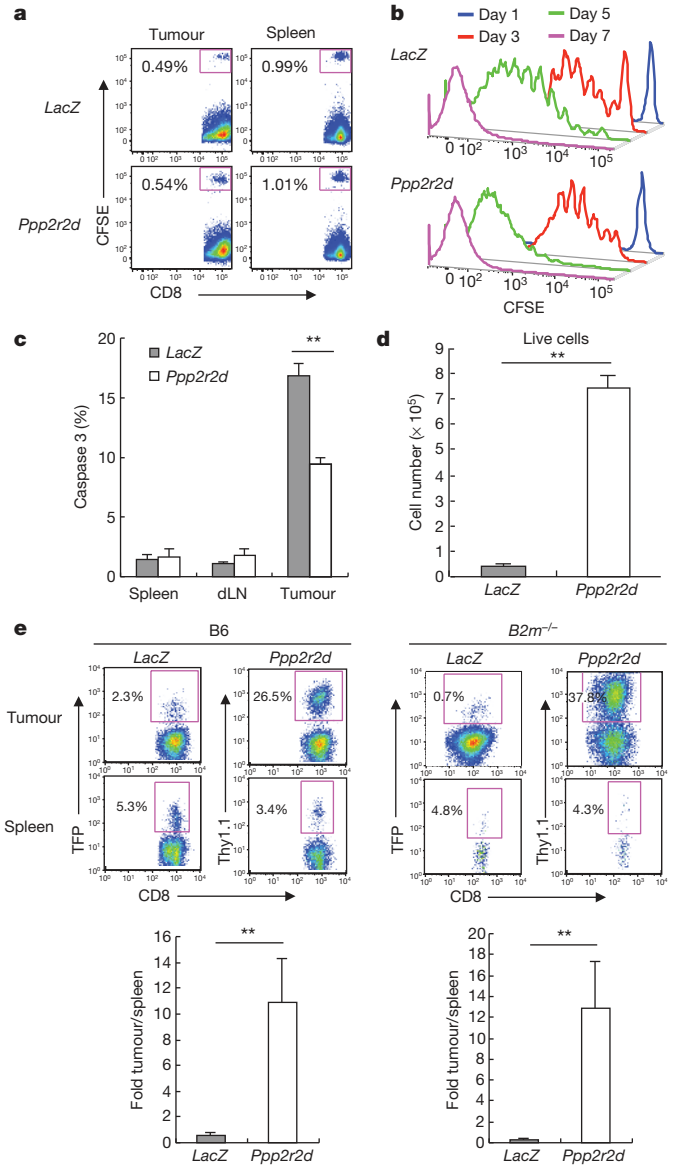

Figure 3 | Changes in T-cell function induced by *Ppp2r2d* shRNA. **a**, Tumour infiltration at 24 h by CFSE-labelled OT-I T cells. **b**, Enhanced proliferation by *Ppp2r2d*-silenced T cells (CFSE dilution). **c**, **d**, Reduced apoptosis by *Ppp2r2d*-silenced OT-I T cell in tumours (**c**, activated caspase-3) or during 3-day co-culture with B16-Ova tumour cells (**d**, annexin V). **e**, *Ppp2r2d*-silencing induced T-cell expansion even when MHC class I expression was restricted to tumour cells; T-cell transfer into C57BL/6 or $B2m^{-/-}$ mice with B16-Ova tumours. Data representative of two independent trials ($n = 3$; $^{**}P \leq 0.01$, two-sided student's *t*-test); mean ± s.d.

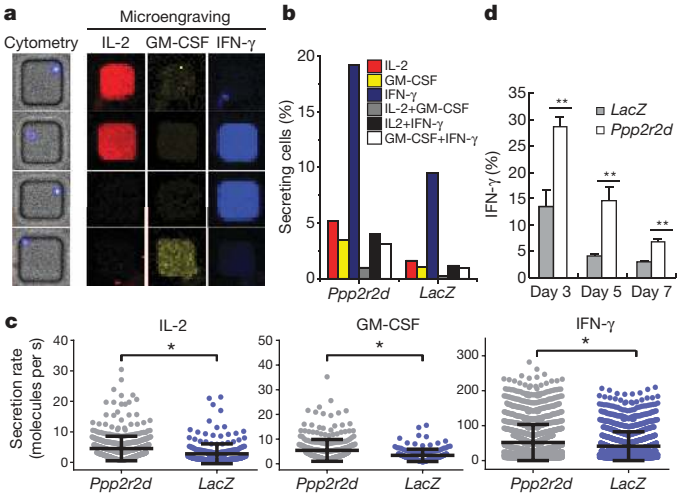

Figure 4 | Cytokine secretion by gene-silenced tumour-infiltrating T cells. **a**–**c**, *Ex vivo* analysis of cytokine production by tumour-infiltrating OT-I T cells at a single-cell level using a nanowell device (84,672 wells of picolitre volume). **a**, Representative single cells in nanowells and corresponding patterns of cytokine secretion. **b**, Percentage of T cells secreting indicated cytokines. **c**, Cytokine secretion rates calculated from standard curves (mean ± s.d., $^{*}P < 0.05$, Mann–Whitney *U*-test). **d**, Intracellular IFN-γ staining for tumour-infiltrating *Ppp2r2d*-silenced T cells, representative of two independent experiments ($n = 3$, $^{**}P \leq 0.01$, two-sided student's *t*-test); mean ± s.d.

for 3 h by CD3/CD28 antibodies on lipid bilayers, followed by 1 h cytokine capture on antibody-coated slides. CD8 T cells showed a higher secretion rate for interferon-γ, interleukin-2 and granulocyte–macrophage colony-stimulating factor (IFN-γ, IL-2 and GM-CSF, respectively) and a larger fraction of T cells secreted more than one cytokine (Fig. 4b, c). The presence of larger numbers of IFN-γ-producing T cells was confirmed by intracellular cytokine staining (Fig. 4d and Extended Data Fig. 5c).

PP2A represents a family of phosphatase complexes composed of catalytic, scaffolding and regulatory subunits. Cellular localization and substrate specificity are determined by one of many regulatory subunits, of which Ppp2r2d is a member[32]. Ppp2r2d directs PP2A to Cdk1 substrates during interphase and anaphase; it thereby inhibits entry into mitosis and induces exit from mitosis[37]. PP2A also has a gatekeeper role for BAD-mediated apoptosis. Phosphorylated BAD is sequestered in its inactive form in the cytosol by 14-3-3, whereas dephosphorylated BAD is targeted to mitochondria where it causes cell death by binding Bcl-X_L and Bcl-2[38]. PP2A phosphatases have also been shown to interact with the cytoplasmic domains of CD28 and CTLA-4 as well as Carma1 (upstream of the NF-κB pathway)[39,40], but it is not known which regulatory subunits are required for these activities. Anti-Ppp2r2d antibodies suitable for the required biochemical studies are not currently available.

Enhanced anti-tumour immunity

Finally, we assessed the ability of a *Ppp2r2d* shRNA to enhance the efficacy of adoptive T-cell therapy. B16-Ova tumour cells (2×10^5) were injected subcutaneously into B6 mice. On day 12, mice bearing tumours of similar size were divided into seven groups, either receiving no T cells, 2×10^6 shRNA-transduced TRP-1 CD4 T cells, 2×10^6 shRNA-infected OT-I CD8 T cells, or both CD4 and CD8 T cells (days 12 and 17). The modest anti-tumour activity of OT-I CD8 T cells (expressing the control *LacZ* shRNA) is consistent with published data[41]. *Ppp2r2d*-silencing improved the therapeutic activity of both CD4 and CD8 T cells (Fig. 5a, b). A *Ppp2r2d* shRNA also enhanced anti-tumour responses when introduced into T cells specific for the endogenous melanoma antigens gp100 (pmel-1 CD8 T cells) and TRP-1 (TRP-1 CD4 T cells) (Fig. 5c). gp100 is a relevant antigen in human melanoma, and a clinical trial in which a gp100-specific TCR (isolated from HLA-A2 transgenic mice) was introduced into peripheral blood T cells demonstrated therapeutic benefit in a subset of patients[42].

Ppp2r2d-silenced T cells acquired an effector phenotype in tumours (Extended Data Fig. 6a) and >30% of the cells expressed granzyme B (Extended Data Fig. 7a). Consistent with greatly increased numbers of such effector T cells in tumours (Extended Data Fig. 7b), terminal deoxynucleotidyl transferase dUTP nick end labelling (TUNEL) demonstrated increased apoptosis in tumours when *Ppp2r2d* rather than *LacZ* shRNA-expressing T cells were present (Extended Data Fig. 7c). B16 melanomas are highly aggressive tumours in part because MHC class I expression is very low. Interestingly, *Ppp2r2d* but not *LacZ* shRNA-expressing T cells significantly increased MHC class I expression (H-$2K^b$) by tumour cells (Extended Data Fig. 7d), possibly due to the observed increase in IFN-γ secretion by T cells (Fig. 4b-d). A

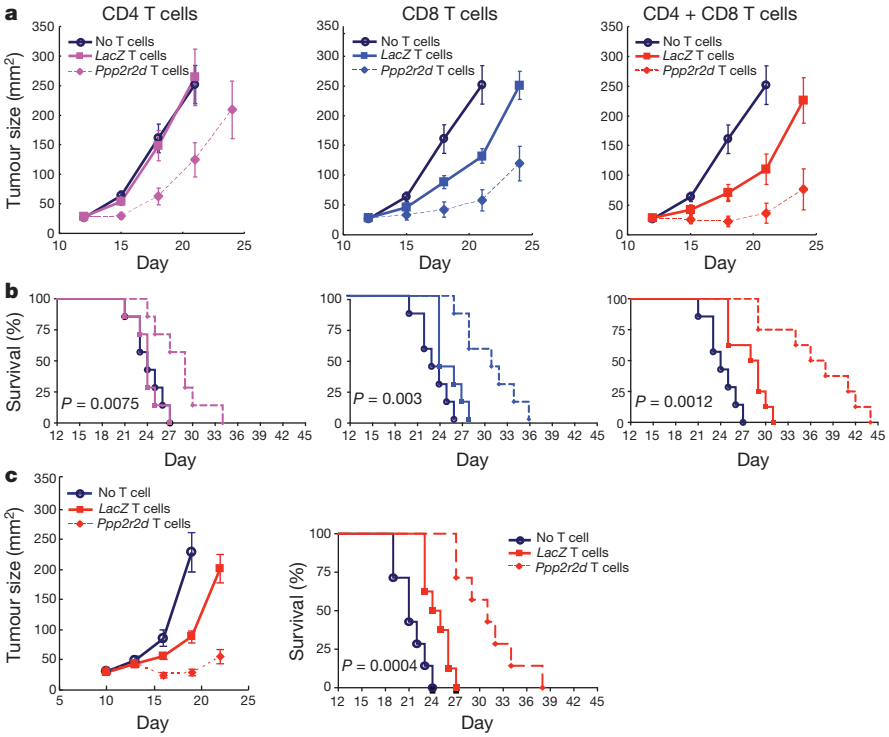

Figure 5 | *Ppp2r2d* silencing enhances anti-tumour activity of CD4 and CD8 T cells. T cells were activated with CD3/CD28 beads and infected with shRNA vectors. **a**, **b**, $CD4^+$ TRP-1 and/or $CD8^+$ OT-I T cells (2×10^6) were transferred (day 12 and 17) into mice bearing day 12 B16-Ova tumours. Tumour burden (**a**) and survival (**b**) were assessed. **c**, $CD4^+$ TRP-1 and $CD8^+$ pmel-1 T cells (3×10^6 each) were transferred (day 10 and 15) into mice with day 10 B16 tumours. Representative of two independent experiments ($n = 7$–9 mice per group), survival analysed using log-rank (Mantel–Cox) test; mean ± s.e.m.

Ppp2r2d shRNA did not reduce expression of inhibitory PD-1 or LAG-3 receptors on tumour-infiltrating T cells, demonstrating that its mechanism of action is distinct from these known negative regulators of T-cell function (Extended Data Fig. 6b). This finding suggests combination approaches targeting these intracellular and cell surface molecules.

Discussion

These results establish the feasibility of *in vivo* discovery of novel targets for immunotherapy in complex tissue microenvironments. We show that it is possible to discover genes with differential action across tissues, as exemplified by T-cell accumulation in tumours compared to secondary lymphoid organs. For genes with tissue-selective action, T-cell proliferation and survival are likely to be under the control of the T-cell receptor and therefore do not occur in tissues lacking presentation of a relevant antigen. Many variations of the approach presented here can be envisioned to investigate control of particular immune cell functions *in vivo*. For example, fluorescent reporters for expression of cytokines or cytotoxic molecules (granzyme B, perforin) could be integrated into our approach to discover genes that control critical T-cell effector functions in tumours.

Targeting of key regulatory switches may offer new approaches to modify the activity of T cells in cancer and other pathologies. For example, recent clinical trials have shown that transfer of genetically modified T cells can result in substantial anti-tumour activity[43–46]. The efficacy of such T-cell-based therapies could be enhanced by shRNA-mediated silencing of genes that inhibit T-cell function in the tumour microenvironment.

METHODS SUMMARY

***In vivo* shRNA screening.** Nine shRNA pools (approximately 5 shRNAs per gene) were created and subcloned into the pLKO-Thy1.1 lentiviral vector. Each pool also included 85 negative-control shRNAs. OT-I T cells were cultured with IL-7 (5 ng ml^{-1}) and IL-15 (100 ng ml^{-1}); on day 2 cells were spin-infected with lentiviral pools supplemented with protamine sulphate (5 μg ml^{-1}) in RetroNectin-coated 24-well plates (5 μg ml^{-1}) at a multiplicity of infection (MOI) of 15. Following infection, OT-1 cells were cultured with IL-7 (2.5 ng ml^{-1}), IL-15 (50 ng ml^{-1}) and IL-2 (2 ng ml^{-1}). On day 5, shRNA-transduced T cells were enriched by positive selection using the Thy1.1 surface reporter (StemCell Technologies). T cells (5×10^6) were injected intravenously into C57BL/6 mice bearing day 14 B16-Ova tumours (15 mice per shRNA pool). Seven days later, shRNA-expressing T cells ($CD8^+V\alpha2^+V\beta5^+Thy1.1^+$) were isolated by flow cytometry from tumours, spleens, tumour-draining lymph nodes and irrelevant lymph nodes. Genomic DNA was purified (Qiagen) and deep-sequencing templates were generated by PCR amplification of the shRNA cassette. Representation of shRNAs in each pool was analysed by deep sequencing using an Illumina Genome Analyzer[47].

Secondary screens were performed using focused pools containing approximately 15 shRNAs per gene as well as 85 negative controls. Cut-off in the secondary screen was defined as ≥ 3 shRNAs with ≥ fourfold enrichment in tumour relative to spleen. Screening results were validated at a cellular level by introducing individual shRNAs into T cells, along with a reporter protein (green, teal, red or ametrine fluorescent proteins, Thy1.1). This approach enabled simultaneous testing of five shRNAs in an animal (three mice per group). Proliferation of shRNA-transduced T cells was visualized on the basis of CFSE dilution after 24 h as well as 3, 5 and 7 days.

Online Content Any additional Methods, Extended Data display items and Source Data are available in the online version of the paper; references unique to these sections appear only in the online paper.

Received 2 April; accepted 31 December 2013.
Published online 29 January 2014.

1. Galon, J. *et al.* Type, density, and location of immune cells within human colorectal tumors predict clinical outcome. *Science* **313,** 1960–1964 (2006).
2. Hamanishi, J. *et al.* Programmed cell death 1 ligand 1 and tumor-infiltrating $CD8^+$ T lymphocytes are prognostic factors of human ovarian cancer. *Proc. Natl Acad. Sci. USA* **104,** 3360–3365 (2007).
3. Mahmoud, S. M. *et al.* Tumor-infiltrating $CD8^+$ lymphocytes predict clinical outcome in breast cancer. *J. Clin. Oncol.* **29,** 1949–1955 (2011).
4. Bindea, G. *et al.* Spatiotemporal dynamics of intratumoral immune cells reveal the immune landscape in human cancer. *Immunity* **39,** 782–795 (2013).
5. Matsushita, H. *et al.* Cancer exome analysis reveals a T-cell-dependent mechanism of cancer immunoediting. *Nature* **482,** 400–404 (2012).
6. Oble, D. A., Loewe, R., Yu, P. & Mihm, M. C. Jr. Focus on TILs: prognostic significance of tumor infiltrating lymphocytes in human melanoma. *Cancer Immun.* **9,** 3 (2009).
7. DuPage, M., Mazumdar, C., Schmidt, L. M., Cheung, A. F. & Jacks, T. Expression of tumour-specific antigens underlies cancer immunoediting. *Nature* **482,** 405–409 (2012).
8. Schreiber, R. D., Old, L. J. & Smyth, M. J. Cancer immunoediting: integrating immunity's roles in cancer suppression and promotion. *Science* **331,** 1565–1570 (2011).

9. Pagès, F. *et al.* In situ cytotoxic and memory T cells predict outcome in patients with early-stage colorectal cancer. *J. Clin. Oncol.* **27,** 5944–5951 (2009).
10. Rusakiewicz, S. *et al.* Immune infiltrates are prognostic factors in localized gastrointestinal stromal tumors. *Cancer Res.* **73,** 3499–3510 (2013).
11. Stumpf, M. *et al.* Intraepithelial CD8-positive T lymphocytes predict survival for patients with serous stage III ovarian carcinomas: relevance of clonal selection of T lymphocytes. *Br. J. Cancer* **101,** 1513–1521 (2009).
12. Gabrilovich, D. I. & Nagaraj, S. Myeloid-derived suppressor cells as regulators of the immune system. *Nature Rev. Immunol.* **9,** 162–174 (2009).
13. Shiao, S. L., Ganesan, A. P., Rugo, H. S. & Coussens, L. M. Immune microenvironments in solid tumors: new targets for therapy. *Genes Dev.* **25,** 2559–2572 (2011).
14. Tanchot, C. *et al.* Tumor-infiltrating regulatory T cells: phenotype, role, mechanism of expansion in situ and clinical significance. *Cancer Microenviron.* **6,** 147–157 (2013).
15. Hodi, F. S. *et al.* Improved survival with ipilimumab in patients with metastatic melanoma. *N. Engl. J. Med.* **363,** 711–723 (2010).
16. Topalian, S. L. *et al.* Safety, activity, and immune correlates of anti-PD-1 antibody in cancer. *N. Engl. J. Med.* **366,** 2443–2454 (2012).
17. Brahmer, J. R. *et al.* Safety and activity of anti-PD-L1 antibody in patients with advanced cancer. *N. Engl. J. Med.* **366,** 2455–2465 (2012).
18. Leach, D. R., Krummel, M. F. & Allison, J. P. Enhancement of antitumor immunity by CTLA-4 blockade. *Science* **271,** 1734–1736 (1996).
19. Wolchok, J. D. *et al.* Nivolumab plus ipilimumab in advanced melanoma. *N. Engl. J. Med.* **369,** 122–133 (2013).
20. Curran, M. A., Montalvo, W., Yagita, H. & Allison, J. P. PD-1 and CTLA-4 combination blockade expands infiltrating T cells and reduces regulatory T and myeloid cells within B16 melanoma tumors. *Proc. Natl Acad. Sci. USA* **107,** 4275–4280 (2010).
21. Westbrook, T. F. *et al.* A genetic screen for candidate tumor suppressors identifies REST. *Cell* **121,** 837–848 (2005).
22. Zender, L. *et al.* An oncogenomics-based *in vivo* RNAi screen identifies tumor suppressors in liver cancer. *Cell* **135,** 852–864 (2008).
23. Luo, B. *et al.* Highly parallel identification of essential genes in cancer cells. *Proc. Natl Acad. Sci. USA* **105,** 20380–20385 (2008).
24. Fidler, I. J. Biological behavior of malignant melanoma cells correlated to their survival *in vivo*. *Cancer Res.* **35,** 218–224 (1975).
25. Hogquist, K. A. *et al.* T cell receptor antagonist peptides induce positive selection. *Cell* **76,** 17–27 (1994).
26. Bellone, M. *et al.* Relevance of the tumor antigen in the validation of three vaccination strategies for melanoma. *J. Immunol.* **165,** 2651–2656 (2000).
27. Overwijk, W. W. *et al.* Tumor regression and autoimmunity after reversal of a functionally tolerant state of self-reactive $CD8^+$ T cells. *J. Exp. Med.* **198,** 569–580 (2003).
28. Paolino, M. & Penninger, J. M. Cbl-b in T-cell activation. *Semin. Immunopathol.* **32,** 137–148 (2010).
29. Zheng, Y., Zha, Y. & Gajewski, T. F. Molecular regulation of T-cell anergy. *EMBO Rep.* **9,** 50–55 (2008).
30. Doody, K. M., Bourdeau, A. & Tremblay, M. L. T-cell protein tyrosine phosphatase is a key regulator in immune cell signaling: lessons from the knockout mouse model and implications in human disease. *Immunol. Rev.* **228,** 325–341 (2009).
31. Tamiya, T., Kashiwagi, I., Takahashi, R., Yasukawa, H. & Yoshimura, A. Suppressors of cytokine signaling (SOCS) proteins and JAK/STAT pathways: regulation of T-cell inflammation by SOCS1 and SOCS3. *Arterioscler. Thromb. Vasc. Biol.* **31,** 980–985 (2011).
32. Barr, F. A., Elliott, P. R. & Gruneberg, U. Protein phosphatases and the regulation of mitosis. *J. Cell Sci.* **124,** 2323–2334 (2011).
33. Muranski, P. *et al.* Tumor-specific Th17-polarized cells eradicate large established melanoma. *Blood* **112,** 362–373 (2008).
34. Koller, B. H., Marrack, P., Kappler, J. W. & Smithies, O. Normal development of mice deficient in beta 2M, MHC class I proteins, and $CD8^+$ T cells. *Science* **248,** 1227–1230 (1990).
35. Torres, A. J., Contento, R. L., Gordo, S., Wucherpfennig, K. W. & Love, J. C. Functional single-cell analysis of T-cell activation by supported lipid bilayer-tethered ligands on arrays of nanowells. *Lab Chip* **13,** 90–99 (2013).
36. Han, Q., Bradshaw, E. M., Nilsson, B., Hafler, D. A. & Love, J. C. Multidimensional analysis of the frequencies and rates of cytokine secretion from single cells by quantitative microengraving. *Lab Chip* **10,** 1391–1400 (2010).
37. Mochida, S., Maslen, S. L., Skehel, M. & Hunt, T. Greatwall phosphorylates an inhibitor of protein phosphatase 2A that is essential for mitosis. *Science* **330,** 1670–1673 (2010).
38. Chiang, C. W. *et al.* Protein phosphatase 2A dephosphorylation of phosphoserine 112 plays the gatekeeper role for BAD-mediated apoptosis. *Mol. Cell. Biol.* **23,** 6350–6362 (2003).
39. Chuang, E. *et al.* The CD28 and CTLA-4 receptors associate with the serine/threonine phosphatase PP2A. *Immunity* **13,** 313–322 (2000).
40. Eitelhuber, A. C. *et al.* Dephosphorylation of Carma1 by PP2A negatively regulates T-cell activation. *EMBO J.* **30,** 594–605 (2011).
41. Tao, J. *et al.* JNK2 negatively regulates $CD8^+$ T cell effector function and anti-tumor immune response. *Eur. J. Immunol.* **37,** 818–829 (2007).
42. Johnson, L. A. *et al.* Gene therapy with human and mouse T-cell receptors mediates cancer regression and targets normal tissues expressing cognate antigen. *Blood* **114,** 535–546 (2009).
43. Brenner, M. K. & Heslop, H. E. Adoptive T cell therapy of cancer. *Curr. Opin. Immunol.* **22,** 251–257 (2010).
44. Turtle, C. J., Hudecek, M., Jensen, M. C. & Riddell, S. R. Engineered T cells for anti-cancer therapy. *Curr. Opin. Immunol.* **24,** 633–639 (2012).
45. Kalos, M. & June, C. H. Adoptive T cell transfer for cancer immunotherapy in the era of synthetic biology. *Immunity* **39,** 49–60 (2013).
46. Restifo, N. P., Dudley, M. E. & Rosenberg, S. A. Adoptive immunotherapy for cancer: harnessing the T cell response. *Nature Rev. Immunol.* **12,** 269–281 (2012).
47. Ashton, J. M. *et al.* Gene sets identified with oncogene cooperativity analysis regulate *in vivo* growth and survival of leukemia stem cells. *Cell Stem Cell* **11,** 359–372 (2012).

Supplementary Information is available in the online version of the paper.

Acknowledgements This work was supported by the National Institutes of Health (Transformative Research Award 1R01CA173750 to K.W.W.), the Melanoma Research Alliance (to K.W.W.), the DF/HCC–MIT Bridge Project and the Lustgarten Foundation (to K.W.W., J.C.L. and H.L.P.), Novartis Institutes of Biomedical Research (to K.W.W.), the Koch Institute Support Grant P30-CA14051 from the National Cancer Institute, the American Cancer Society John W. Thatcher, Jr Postdoctoral Fellowship in Melanoma Research (to D.R.S.), the Terri Brodeur Breast Cancer Foundation Postdoctoral Fellowship (to P.Z.) and a NIH T32 grant (AI07386 to D.A.A.A.).

Author Contributions K.W.W., P.Z., S.J.T., G.D. and H.C. contributed to the overall study design; K.W.W., P.Z. and D.R.S. designed experiments; P.Z., D.A.A.A. and H.C. developed procedure for lentiviral infection of T cells and optimized approaches for adoptive T-cell therapy; P.Z., D.R.S. and D.A.A.A. performed shRNA screen; G.S.C., D.E.R. and N.H. provided pooled shRNA library and advice on shRNA screen; Y.N. and G.D. provided B16-Ova cell line and advice on tumour model; A.J.T. and J.C.L. performed nano-well analysis of cytokine production, V.C. and S.J.T. performed histological studies, W.P. performed protein quantification by mass spectrometry, S.K.D. and H.L.P. provided mouse models; J.B., K.E. and J.L. performed microarray analysis; K.W.W., P.Z. and D.R.S. wrote the paper.

Author Information The access number for microarray data is GSE53388 in the Genomic Spatial Event (GSE) database. Reprints and permissions information is available at www.nature.com/reprints. The authors declare competing financial interests: details are available in the online version of the paper. Readers are welcome to comment on the online version of the paper. Correspondence and requests for materials should be addressed to K.W.W. (kai_wucherpfennig@dfci.harvard.edu).

METHODS

***In vivo* shRNA screening.** The study design was approved by the institutional animal care and use committee (IACUC). shRNAs targeting 255 genes over-expressed in dysfunctional T cells (anergic or exhausted state) and 1,307 kinase/phosphatase genes (approximately 5 shRNAs per gene) were obtained from The RNAi Consortium. Nine pools were created with shRNAs subcloned into the pLKO-Thy1.1 lentiviral vector. Each pool also contained 85 negative-control shRNAs (number of shRNAs: green fluorescent protein (GFP), 24; *LacZ*, 20; luciferase, 25; red fluorescent protein (RFP), 16). OT-I T cells isolated by negative selection (StemCell Technologies) were cultured with IL-7 (5 ng ml^{-1}, Peprotech) and IL-15 (100 ng ml^{-1}, Peprotech) in complete RPMI media (RPMI 1640, 10% FBS, 20 mM HEPES, 1 mM sodium pyruvate, 0.05 mM 2-mercaptoethanol, 2 mM L-glutamine, 100 μg ml^{-1} streptomycin and 100 μg ml^{-1} penicillin). On day 2, OT-I T cells (2×10^6 per well) were spin-infected with lentiviral pools supplemented with protamine sulphate (5 μg ml^{-1}) in 24-well plates coated with RetroNectin (5 μg ml^{-1}) at a multiplicity of infection (MOI) of 15. Typically approximately 50×10^6 OT-1 T cells were infected for each pool. Following infection, OT-I cells were cultured with IL-7 (2.5 ng ml^{-1}), IL-15 (50 ng ml^{-1}) and IL-2 (2 ng ml^{-1}, BioLegend) in complete RPMI media. On day 5, live cells were enriched using a dead cell removal kit (Miltenyi), and infected cells (20–25% Thy1.1$^+$) were positively selected based on the Thy1.1 marker (StemCell Technologies) to 50–60% Thy1.1 positivity. T cells (5×10^6) were injected intravenously into C57BL/6 mice bearing day 14 B16-Ova tumours (2×10^5 tumour cells injected on day 0), 15 mice per shRNA pool (number of animals chosen to provide sufficient cells for T cell isolation and PCR). Genomic DNA was isolated from 5×10^6 enriched OT-I cells as the start population for deep sequencing. Seven days later, shRNA-expressing T cells (CD8$^+$Vα2$^+$Vβ5$^+$Thy1.1$^+$) were isolated by flow cytometry from tumours, spleens, tumour-draining lymph nodes and irrelevant lymph nodes. Genomic DNA was isolated (Qiagen) and deep-sequencing templates were generated by PCR of the shRNA cassette. Representation of shRNAs in each pool was analysed by deep sequencing using an Illumina Genome Analyzer[47]. Data were normalized using the average reads of control shRNAs in each pool. Kinase/phosphatase genes were selected for the secondary screen based on expression levels in T cells (Immunological Genome Project, http://www.immgen.org/). For the secondary screen, approximately 10 additional shRNAs were synthesized for each gene (IDT) for a total of approximately 15 shRNAs per gene. These focused pools contained 85 negative-control shRNAs. Two control shRNAs (one for RFP, one for luciferase) showed some enrichment in tumours relative to spleen (4.0 and 5.1-fold, respectively). Cut-off in the secondary screen was defined as ≥ 3 shRNAs, with ≥ fourfold enrichment in tumours relative to spleen. Data from primary and secondary screens are provided in Supplementary Table 1.

T-cell isolation from tumours. B16-Ova melanomas were cut into small pieces in Petri dishes containing 5 ml of PBS, 2% FBS and washed with PBS. Tumours were resuspended in 15 ml RPMI supplemented with 2% FBS, 50 U ml^{-1} collagenase type IV (Invitrogen), 20 U ml^{-1} DNase (Roche); samples were incubated at 37 °C for 2 h, and tissue was further dissociated using a gentleMACS Dissociator (Miltenyi Biotech). Suspensions were washed three times with PBS and passed through a 70 μm strainer. Lymphocytes were isolated by density gradient centrifugation and then either analysed or sorted by flow cytometry using a FACSAria (BD Biosciences).

Quantification of T-cell enrichment in tumours by flow cytometry. Individual shRNAs were cloned into lentiviral vectors encoding five different reporter proteins (GFP, teal fluorescent protein (TFP), RFP or ametrine fluorescent proteins, Thy1.1). Cytokine-pretreated OT-I T cells were transduced with lentiviral vectors driving expression of a single shRNA/reporter; 1×10^6 T cells of each population were mixed and co-injected intravenously into C57BL/6 mice bearing day 14 B16-Ova tumours. Seven days later, T-cell populations were identified by flow cytometry based on co-introduced reporters. Fold-enrichment in tumours compared to spleen was calculated based on the percentage of OT-I T cells in each organ expressing a particular reporter. In other experiments, 2×10^6 OT-I CD8 or TRP-1 CD4 T cells were transduced with lentiviral vectors encoding *Ppp2r2d* or *LacZ* shRNAs (Thy1.1 reporter) and injected into mice bearing day 14 B16-Ova (for OT-I T cells) or B16 (for TRP-1 T cells) tumours. On day 7, absolute numbers of shRNA-expressing T cells were determined in tumours and spleens.

T-cell migration, proliferation and cytokine secretion. OT-I T cells expressing *LacZ* or *Ppp2r2d* shRNAs were purified using the Thy1.1 reporter and cultured in complete RPMI media without added cytokines for 24 h. Live cells isolated by Ficoll density gradient centrifugation (Sigma) were labelled with CFSE (carboxyfluorescein diacetate, succinimidyl ester, Invitrogen), and 2×10^6 labelled cells were injected into mice bearing day 14 B16-Ova tumours. CFSE dilution was quantified by flow cytometry at 24 h as well as days 3, 5 and 7 following transfer. In addition, intracellular staining was performed on days 3, 5 and 7 for IFN-γ, TNF-α and isotype controls (BD).

T-cell apoptosis. Cytokine pre-treated OT-I cells were transduced with *LacZ* or *Ppp2r2d* shRNAs and injected into mice bearing day 14 B16-Ova tumours. After 7 days, intracellular staining was performed using an activated caspase 3 antibody (Cell Signaling) and CD8/Thy1.1 double-positive T cells were gated in the FACS analysis.

Treatment of tumours by adoptive T-cell transfer. B16-Ova cells (2×10^5) were injected subcutaneously into female C57BL/6 mice (10 weeks of age). On day 12, mice bearing tumours of similar size were divided into 7 groups (7–9 mice per group). Anti-CD3/CD28 bead activated CD4 TRP-1 or/and CD8 OT-I T cells infected with *Ppp2r2d* or *LacZ* shRNA vectors (2×10^6 T cells each) were injected intravenously on days 12 and day 17. For the treatment of B16 tumours, mice were treated at day 10 with anti-CD3/CD28 bead activated CD4 TRP-1 and CD8 pmel-1 T cells expressing *Ppp2r2d* or *LacZ* shRNAs ($3x10^6$ T cells each). Tumour size was measured every three days following transfer and calculated as length × width. Mice with tumours ≥ 20 mm on the longest axis were euthanized.

Quantification of Ppp2r2d protein levels by mass spectrometry. A previously reported approach for absolute quantification (AQUA) of proteins from cell lysates by mass spectrometry was used to measure the effect of *Ppp2r2d* shRNA expression at the protein level[48]. This strategy was based on a 'selective reaction monitoring' approach in which a synthetic peptide with incorporated stable isotopes was used as an internal standard for mass spectrometry analysis. OT-I cells expressing *LacZ* or *Ppp2r2d* shRNAs were sorted to purity using FACS. Cells (1×10^6) were lysed in 1 ml of MPER extraction reagent (Pierce) containing a protease inhibitor cocktail (Sigma), 1 mM EDTA and 1 mM PMSF for 15 min on ice with occasional vortexing. Cell debris was removed by centrifugation and the protein supernatant was filtered (0.2-μm SpinX centrifuge filter, Costar). Protein concentration was determined by Bradford assay (Bio-Rad) and ultraviolet 280-nm analysis (NanoDrop instrument); 0.1 mg of cellular protein was separated by SDS–PAGE and stained with Coomassie blue reagent (Pierce). Gel bands corresponding to a MW range of 45-60 kDa were excised followed by in-gel digestion of proteins with trypsin. Eluted peptides were spiked with 300 fmol of isotopically labelled Ppp2r2d (FFEEPEDPSS [13C-15N-R]-OH) and Actin B (GYSFTTTAE[13C-15N-R]-OH) peptides (21st Century Biochemicals) for quantification by LC-MS/MS (LTQ XL Orbitrap, Thermo Scientific). The Ppp2r2d peptide was chosen from a region of the protein that differs from other regulatory subunits of PP2A. Initially, a LC-MS/MS run of a *LacZ* shRNA sample was analysed to localize the Ppp2r2d and Actin B peptides that were being monitored. The AQUA peptides co-eluted with the corresponding endogenous peptides from the reverse-phase column, yet their higher molecular mass (10 Da) enabled the ratio of peak intensity for endogenous and AQUA peptides to be determined using abundant peptide fragment ions. Triplicate samples were analysed by SDS–PAGE followed by LC–MS/MS and statistical significance was determined using GraphPad Prism 6.0 software using a two-sided Student's *t*-test (*F* test, $*P = 0.0062$).

48. Gerber, S. A., Rush, J., Stemman, O., Kirschner, M. W. & Gygi, S. P. Absolute quantification of proteins and phosphoproteins from cell lysates by tandem MS. *Proc. Natl Acad. Sci. USA* **100,** 6940–6945 (2003).

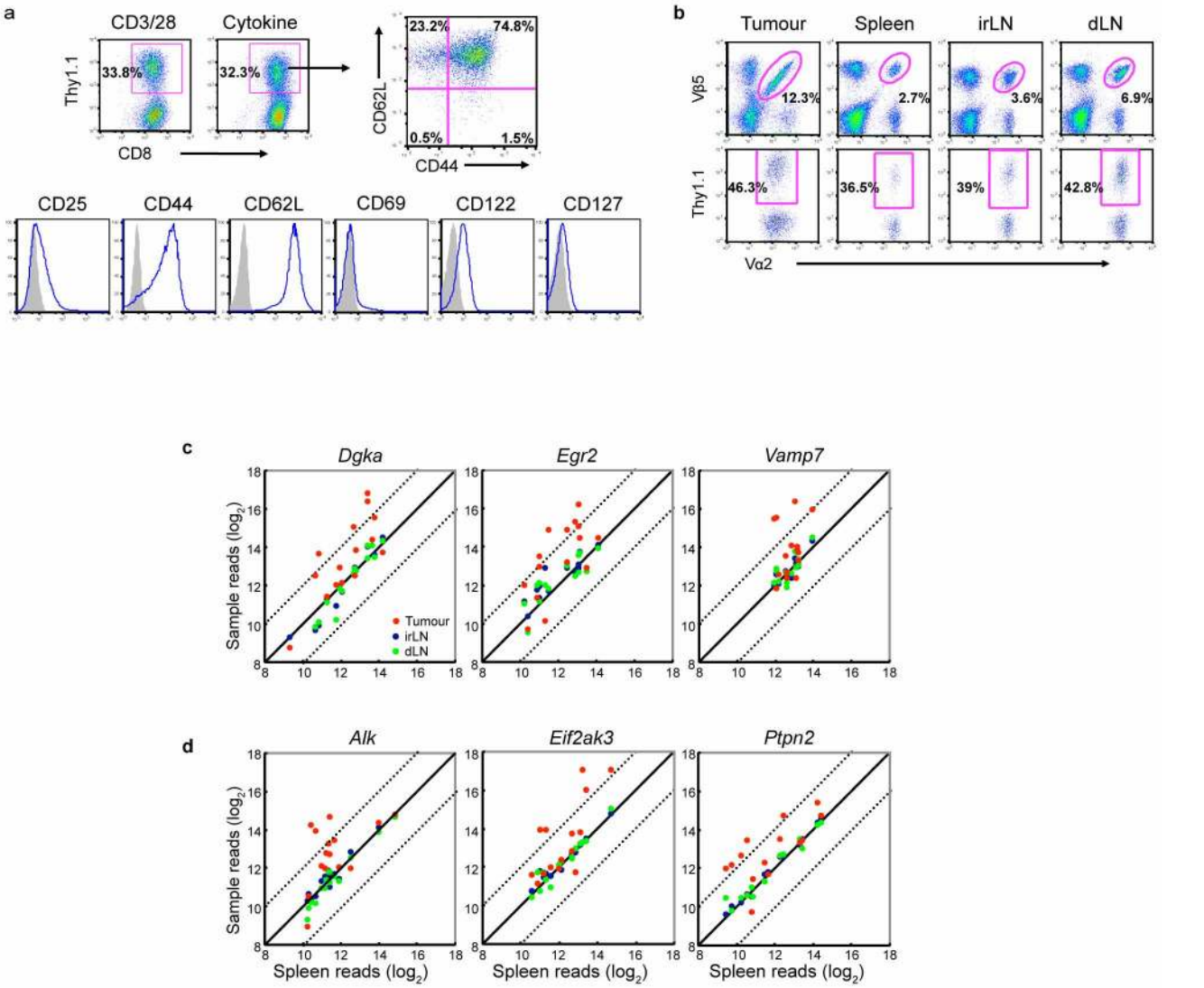

Extended Data Figure 1 | *In vivo* RNAi screening procedure. **a**, Infection of $CD8^+$ T cells from $Rag1^{-/-}$/OT-I TCR transgenic mice with shRNA pools. T cells were either activated with anti-CD3/CD28 beads or exposed to recombinant murine IL-7/IL-15 for 48 h. T cells were then infected with a *LacZ* control shRNA lentiviral vector and cultured for an additional three days. Transduction efficiency was determined based on expression of the Thy1.1 reporter encoded by the lentiviral vector. Cytokine-cultured T cells expressing the *LacZ* control shRNA were then stained with a panel of activation markers (blue lines; isotype control, shaded). The majority of infected T cells showed a central memory phenotype ($CD62L^+CD44^+$). **b**, Representative flow cytometry plots of OT-I T cells sorted from tumours and secondary lymphoid organs for deep sequencing analysis (dLN, tumour-draining lymph node; irLN, irrelevant lymph node). $CD8^+V\alpha2^+V\beta5^+Thy1.1^+$ cells were sorted and genomic DNA was extracted for PCR amplification of the shRNA cassette. **c**, Deep sequencing results from T-cell dysfunction screen. shRNA sequencing reads for genes positive in secondary screen are plotted in comparison to spleen for tumours (red), irrelevant lymph nodes (irLN, blue) and tumour-draining lymph nodes (dLN, green), with dashed lines indicating a deviation of $\log_2$ from the diagonal. Data show enrichment of particular shRNAs representing these genes in tumours compared to spleens or lymph nodes. **d**, Deep sequencing results from kinase and phosphatase screen, as described in **c**.

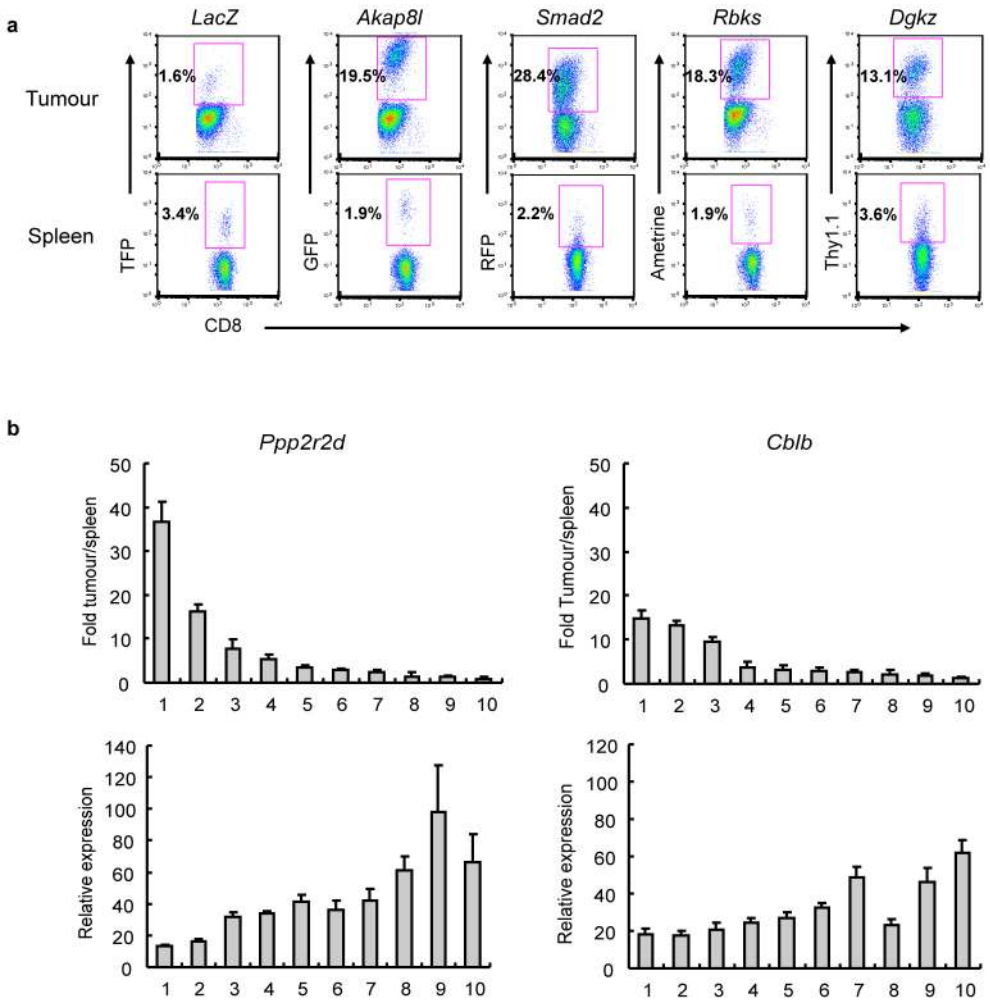

Extended Data Figure 2 | Validation of shRNAs from *in vivo* RNAi screen. **a**, FACS-based analysis of T-cell enrichment in tumours. Positive shRNAs from deep sequencing analysis were cloned into vectors driving expression of one of four distinct fluorescent proteins (TFP, GFP, RFP, ametrine) or Thy1.1. OT-I T cells were transduced with shRNA vectors and the five populations of T cells (normalized for transduction efficiency) were co-injected into B16-Ova tumour-bearing mice. T cells were isolated from tumours and spleens on day 7, and the percentage of reporter-positive $CD8^+V\alpha2^+V\beta5^+$ T cells was determined by flow cytometry. **b**, FACS analysis of T-cell enrichment in tumours compared to spleen (as described above) for cells expressing a panel of *Ppp2r2d* or *Cblb* shRNAs (upper panels). Also, *Ppp2r2d* and *Cblb* mRNA levels were measured by qPCR before T-cell transfer (lower panels). The strongest T-cell enrichment in tumours was observed for shRNAs with >80% knockdown efficiency at the mRNA level (shRNAs 1 and 2 for both *Ppp2r2d* and *Cblb*). Data represent biological replicates ($n = 3$), each value represents mean ± s.d.

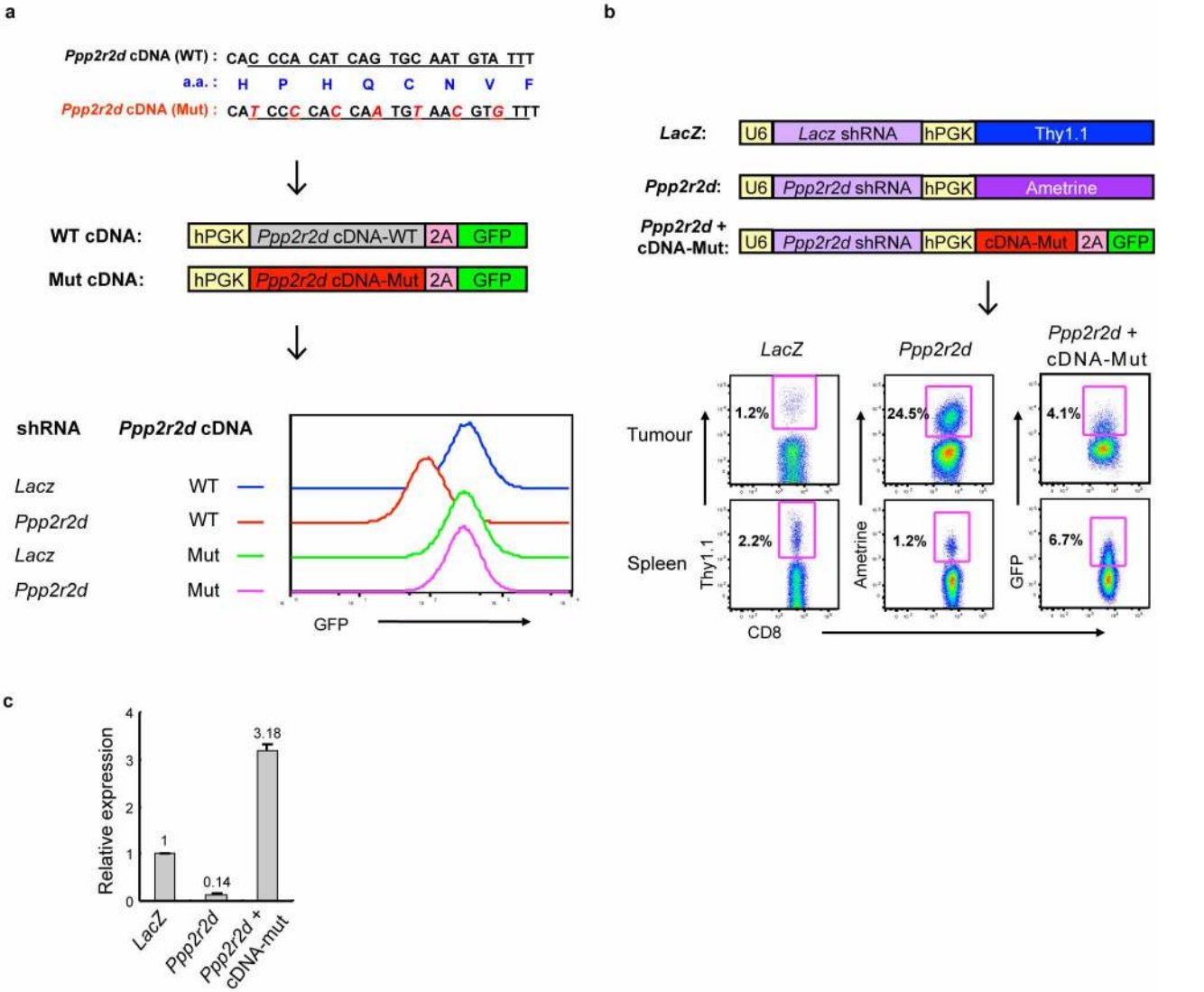

Extended Data Figure 3 | Specificity of *Ppp2r2d* shRNA. **a**, Generation of mutant *Ppp2r2d* cDNA with wild-type protein sequence but disrupted shRNA binding site. Both mutant and wild-type *Ppp2r2d* cDNAs were cloned into a modified pLKO.3G vector with a 2A peptide ribosomal skip sequence and GFP. This approach resulted in stoichiometric expression of Ppp2r2d protein and GFP in EL4 thymoma cells. GFP-expressing EL4 cells were sorted to purity and transduced with *LacZ* or *Ppp2r2d* shRNA vectors expressing a Thy1.1 reporter. shRNA-transduced (Thy1.1$^+$) cells were analysed by flow cytometry for GFP expression. The *Ppp2r2d* shRNA reduced GFP levels when wild-type *Ppp2r2d* cDNA, but not when mutant *Ppp2r2d* cDNA was co-expressed. **b**, Expression of *Ppp2r2d* mutant cDNA prevents phenotype induced by *Ppp2r2d* shRNA. OT-I T cells were transduced with a vector encoding *LacZ* shRNA, *Ppp2r2d* shRNA or *Ppp2r2d* shRNA plus mutant *Ppp2r2d* cDNA. The different T-cell populations were normalized for transduction efficiency and co-injected into B16-Ova tumour-bearing mice. The percentage of each T-cell population in tumours and spleens was quantified by gating on CD8$^+$Vα2$^+$Vβ5$^+$ T cells; transduced cells were detected based on expression of Thy1.1 or ametrine/GFP fluorescent reporters (representative data from 2 independent experiments, $n = 3$ mice per experiment). **c**, qPCR analysis for *Ppp2r2d* expression in OT-I T cells transduced with *LacZ* shRNA, *Ppp2r2d* shRNA, and *Ppp2r2d* shRNA plus *Ppp2r2d* mutant cDNA. Data represent biological replicates ($n = 3$), each value represents mean ± s.d.

a

Gene Symbol	Function	Enrichment Fold
Ppp2r2d	Regulatory subunit of PP2A phosphatase	17.2
Arhgap5	Negative regulator of Rho GTPases	15.7
Alk	Anaplastic lymphoma kinase (translocation of nucleophosmin and ALK in ALCL)	13.5
Egr2	Transcription factor involved in T cell unresponsiveness, expression of Cblb	10.2
Ptpn2	Inhibitor of T cell and cytokine signaling	7.4

b

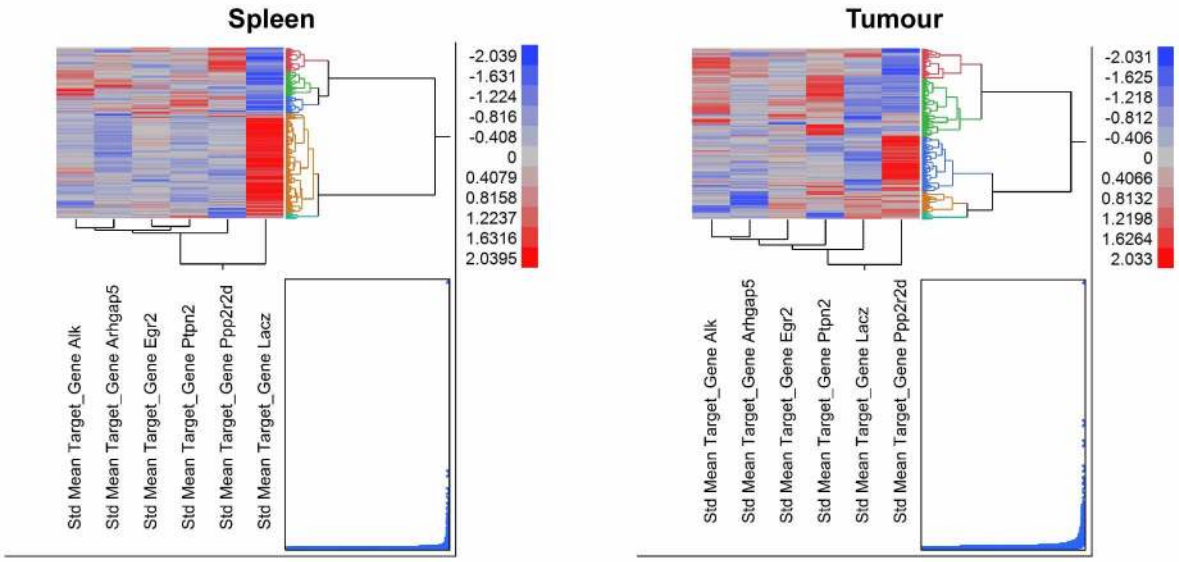

c

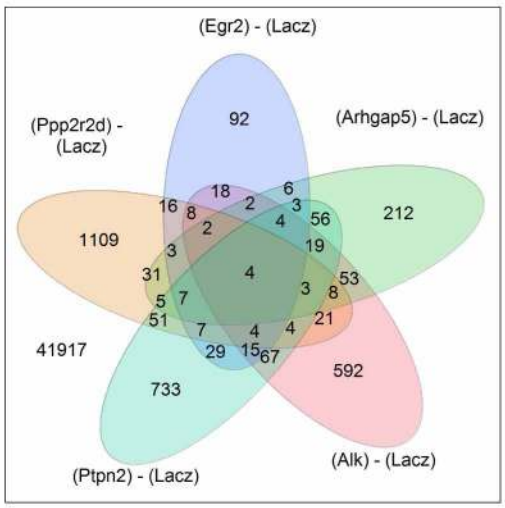

	Alk	*Arhgap5*	*Egr2*	*Ppp2r2d*	*Ptpn2*
Alk		1.0E-31	5.6E-14	ns	1.9E-23
Arhgap5			7.8E-07	9.5E-14	3.5E-16
Egr2				3.2E-08	3.3E-24
Ppp2r2d					1.6E-07
Ptpn2					

Extended Data Figure 4 | Expression profiles of gene-silenced CD8 T cells in tumours. OT-I T cells were transduced with lentiviral vectors driving expression of one of five experimental shRNAs or *LacZ* control shRNA. T cells were injected into day 14 B16-Ova tumour-bearing mice and isolated from tumours and spleens 7 days later. Cells were sorted to high purity and total RNA was obtained for Affymetrix gene expression profiling. For each shRNA, arrays were performed in triplicate (6 mice per group). **a**, Two genes (*Egr2* and *Ptpn2*) have known functions in T cells. Enrichment in tumour versus spleen was calculated based on deep sequencing results from the secondary screen. **b**, Clustering of mean expression levels for mRNAs found to be significantly regulated by T cells in spleens or tumours expressing the *LacZ* control shRNA or one of five experimental shRNAs. Significant expression differences were defined as an ANOVA P value ≤ 0.01 between T cells expressing *LacZ* control shRNA or one of five experimental shRNAs (*Alk*, *Arhgap5*, *Egr2*, *Ptpn2* or *Ppp2r2d*) (JMP-Genomics 6.0, SAS Institute). mRNAs significantly regulated in one or more treatment groups are shown after clustering (fast Ward). **c**, Venn diagram showing overlaps between expression signatures by tumour-infiltrating T cells transduced with one of the five experimental shRNAs (signatures defined as an ANOVA $P \leq 0.01$ as described above). Indicated are the numbers of overlapping probe IDs for any combination of the 5 signatures, as indicated by the overlapping ovals. The significance of the overlaps versus those expected by random chance (Fisher's exact test) is shown in the accompanying table.

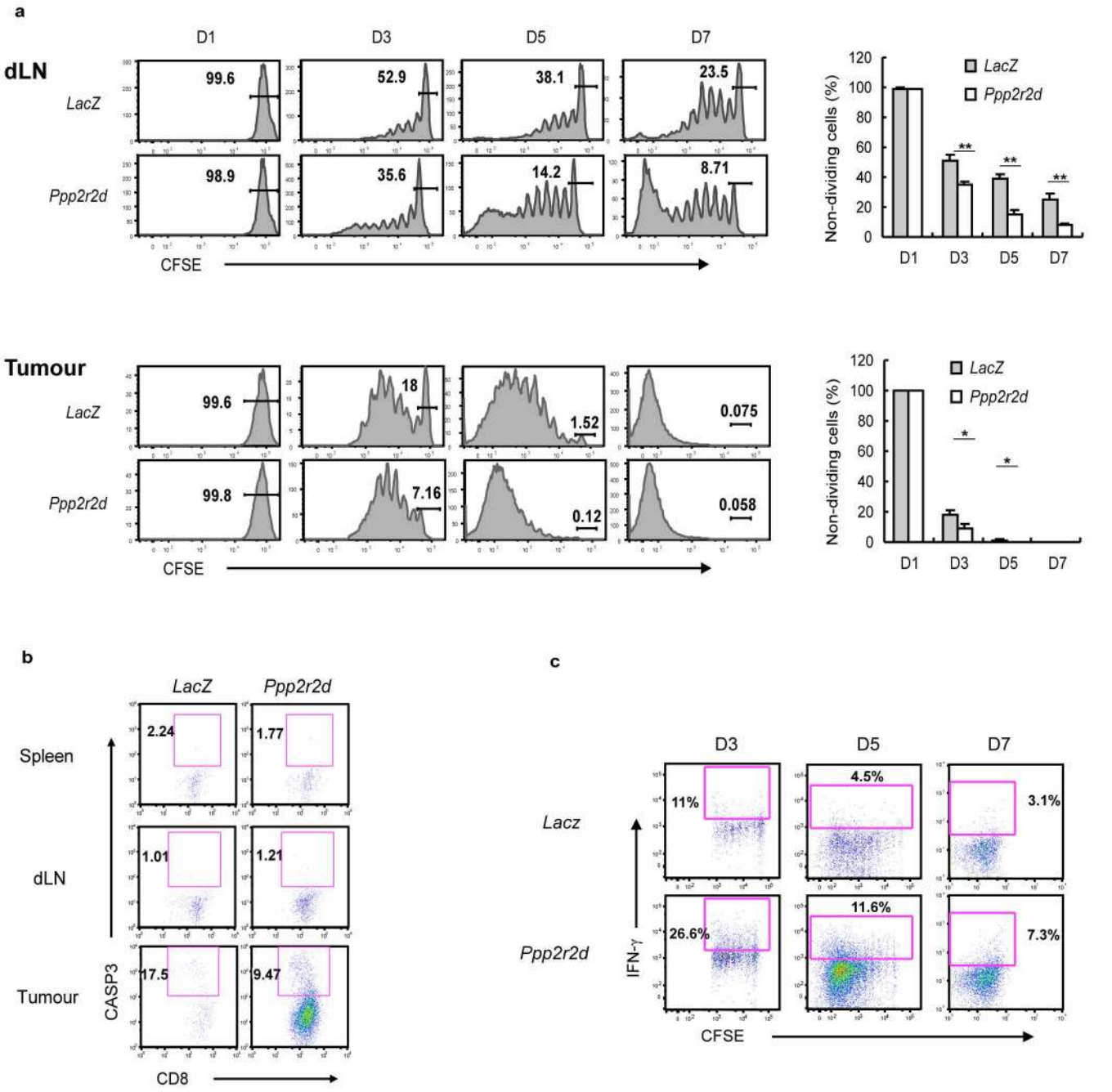

Extended Data Figure 5 | *Ppp2r2d* shRNA enhances T-cell proliferation and reduces apoptosis. **a**, Proliferation of *Ppp2r2d* shRNA-expressing T cells in tumours and tumour-draining lymph nodes. OT-I T cells expressing *Ppp2r2d* or *LacZ* shRNAs were labelled with CFSE and injected into B16-Ova tumour-bearing mice. T cells were isolated from the indicated organs on days 1, 3, 5 and 7 to examine the extent of T-cell proliferation based on CFSE dilution. T cells that had not diluted CFSE (non-dividing cells) were quantified (right). **b**, Viability of tumour-infiltrating T cells. OT-I T cells expressing *Ppp2r2d* or *LacZ* shRNAs were injected into B16-Ova tumour-bearing mice. T cells were isolated on day 7 and apoptosis was assessed by intracellular staining with an antibody specific for activated caspase-3 (some T-cell death may have been caused by the isolation procedure from tumours). **c**, Intracellular cytokine staining for IFN-γ by *LacZ* and *Ppp2r2d* shRNA-expressing T cells collected from B16-Ova tumours (primary flow cytometry analysis for data summarized in Fig. 4d); T cells were labelled with CFSE before injection. Data for all experiments are representative of two independent trials. Statistical analysis was performed on biological replicates ($n = 3$); $^{*}P \leq 0.05$, $^{**}P \leq 0.01$, two-sided Student's *t*-test. Each value represents mean ± s.d.

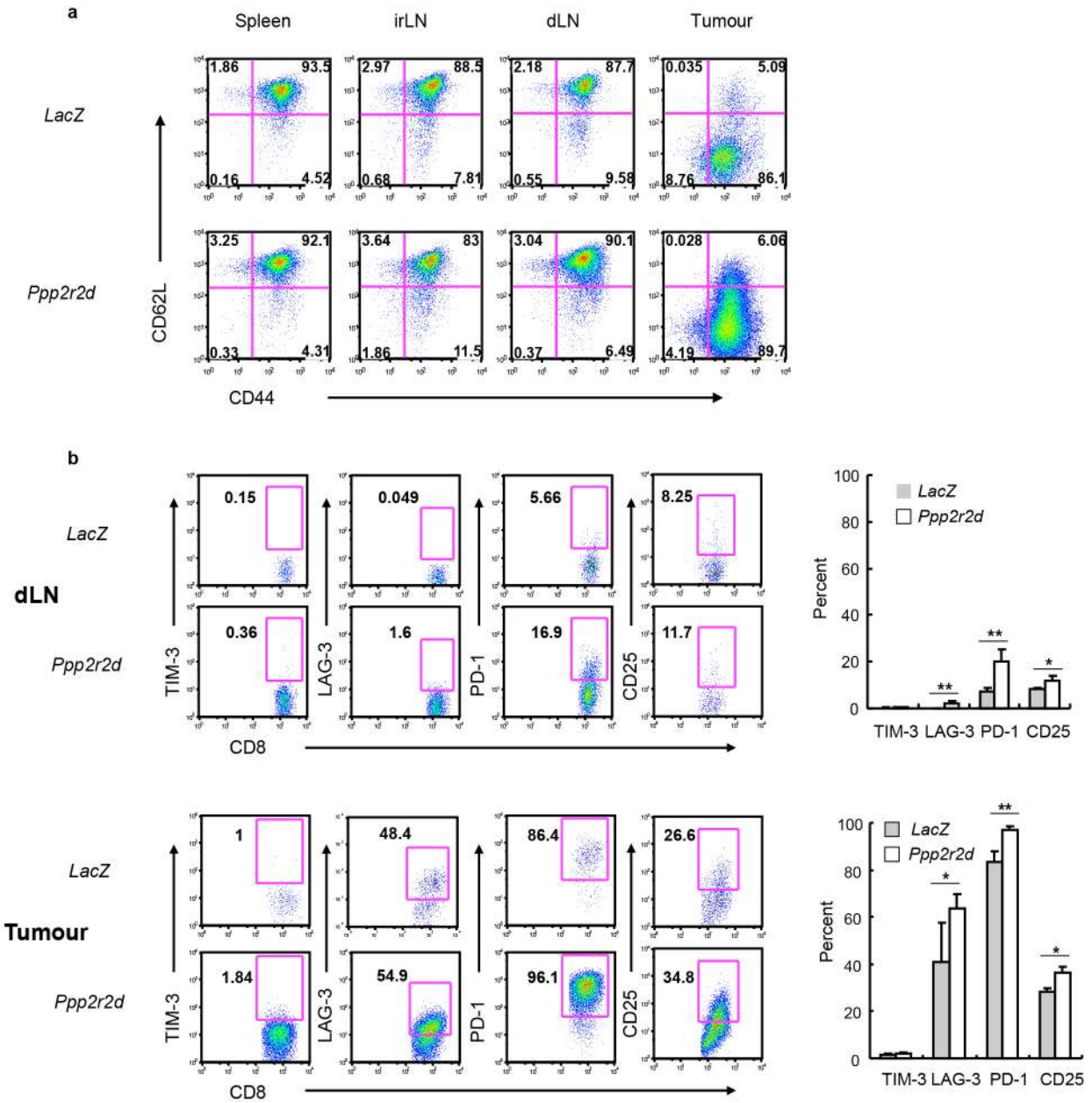

Extended Data Figure 6 | Phenotypic characterization using memory, activation and exhaustion markers. **a**, The majority of adoptively transferred OT-I cells have a memory phenotype in lymph nodes but an effector phenotype in tumours. Cytokine pre-treated cells expressing *Ppp2r2d* or *LacZ* shRNAs were injected into mice bearing day 14 B16-Ova tumours. On day 7 following transfer, T cells were collected from the indicated organs and stained with CD62L and CD44 antibodies. FACS analysis of shRNA-expressing OT-I cells was performed by gating on CD8/Thy1.1 double-positive cells. **b**, Analysis of exhaustion markers. OT-I cells were collected from draining lymph nodes and tumours of mice and stained with antibodies specific for TIM-3, LAG-3, PD-1 and CD25. For all experiments ($n = 3$ biological replicates; $^{*}P \leq 0.05$, $^{**}P \leq 0.01$, two-sided Student's *t*-test); each value represents mean ± s.d.

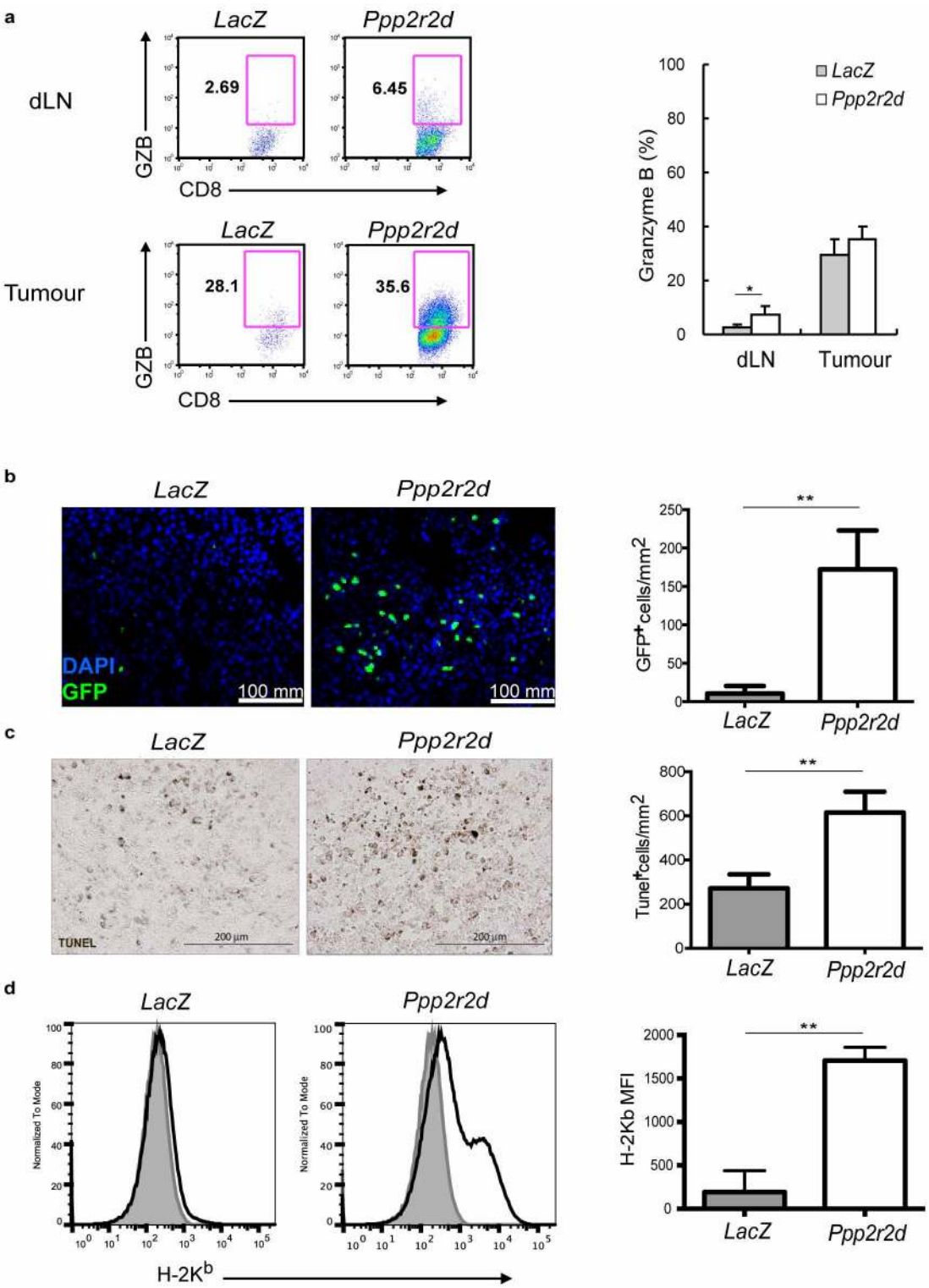

Extended Data Figure 7 | Mechanisms of anti-tumour activity of *Ppp2r2d*-silenced T cells. **a**, Intracellular staining for granzyme B by OT-I T cells in tumour-draining lymph nodes and tumours. **b**, Infiltration of shRNA-expressing T cells into tumours. OT-I T cells were transduced with *LacZ* or *Ppp2r2d* shRNA vectors encoding a GFP reporter and injected into B16-Ova tumour-bearing mice. After 7 days, tumours were excised and frozen sections stained with anti-GFP and DAPI to enumerate shRNA-expressing OT-I T cells in tumours. **c**, Tumour cell apoptosis. TUNEL immunohistochemistry was performed on tissue sections and apoptotic cells were quantified. **d**, MHC class I expression by tumour cells. Tumours were digested with collagenase and stained with CD45.2 and H-2K^b antibodies. FACS analysis for H-2K^b expression was performed by gating on CD45.2-negative melanoma cells. Data represent biological replicates ($n = 3$), each value represents mean ± s.d.

Extended Data Table 1 | Tumour-enriched shRNAs from secondary screen

a

	Symbol	Total # shRNAs	Enrichment (fold)	Function
1	*Dgkz*	6	5.2 - 14.0	Phosphorylates and thereby inactivates DAG
2	*Egr2*	6	4.0 - 10.2	Transcription factor involved in T cell unresponsiveness, expression of Cblb
3	*Smad2*	5	6.7 - 30.3	TGF beta signaling pathway
4	*Cblb*	5	4.1 - 10.8	E3 ubiquitin ligase (degradation of TCR and signaling molecules; ko mice reject tumours
5	*Inpp5b*	5	4.3 - 9.5	Inositol polyphosphate-5-phosphatase, hydrolyzes PIP2
6	*Socs1*	5	4.1 - 8.5	Inhibitor of cytokine signaling
7	*Jun*	5	5.2 - 6.4	Persistent AP-1 activation in tumour-infiltrating T cells leads to upregulated PD-1
8	*Vamp7*	4	4.0 - 11.3	Vesicle associated transmembrane protein
9	*Dgka*	4	5.0 - 10.2	Phosphorylates and thereby inactivates DAG
10	*Mdfic*	4	4.4 - 10.0	Inhibits viral gene expression, interacts with cyclin T1 and T2
11	*Nptxr*	4	4.0 - 7.2	Pentraxin receptor
12	*Socs3*	4	4.6 - 6.3	Inhibitor of cytokine signaling
13	*Entpd1*	3	6.5 - 13.3	Extracellular degradation of ATP to AMP (an inhibitory signal through AMP kinase)
14	*Pdz1ip1*	3	4.8 - 12.9	Pdzk1 interacting protein, expression correlates with tumour progression
15	*F11r*	3	4.6 - 6.8	Cell migration
16	*Fyn*	3	4.1 - 6.5	Inhibits activation of resting T cells (through Csk)
17	*Ypel2*	3	4.6 - 5.1	Function unknown

b

	Symbol	Total # shRNAs	Enrichment (fold)	Function
1	*Rbks*	6	4.0 - 12.8	Ribokinase, carbohydrate metabolism
2	*Pkd1*	6	4.9 - 9.9	Cell cycle arrest (activates JAK/STAT pathway)
3	*Ppp2r2d*	5	4.0 - 17.2	Regulatory subunit of PP2A phosphatase
4	*Eif2ak3*	5	4.8 - 13.4	ER stress sensor, resistance of cancer cells to chemotherapy
5	*Ptpn2*	5	4.7 - 7.4	Inhibitor of T cell and cytokine signaling
6	*Hipk1*	4	4.5 - 12.3	Interacts with p53 and c-myb, knockout mice develop fewer carcinogen-induced tumours
7	*Grk6*	4	4.2 - 11	Regulator of particular G-protein coupled receptors
8	*Cdkn2a*	4	4.1 - 7.2	G1 cell cycle arrest and apoptosis in T cells
9	*Sbf1*	4	4.8 - 6.9	Activates MTMR2, which dephosphorylates PI(3)P and PI(3,5)P2
10	*Ipmk*	4	4.0 - 6.9	Inositol polyphosphate kinase, nuclear functions such as chromatin remodeling
11	*Rock1*	4	4.1 - 6.5	Rho kinase, inhibitors have shown activity in mouse models of cancer
12	*Stk17b*	4	4.0 - 6.4	Inhibitor of T cell signaling forms complex with protein kinase D
13	*Mast2*	4	4.1 - 5.1	Microtubule-associated serine/threonine kinase
14	*Arhgap5*	3	6.0 - 15.7	Negative regulator of Rho GTPases, inhibition can reduce cancer cell invasion
15	*Alk*	3	9.6 - 13.5	Anaplastic lymphoma kinase (translocation of nucleophosmin and ALK in ALCL)
16	*Nuak*	3	4.5 - 13.1	Member of AMP-activated protein kinase-related kinase family, oncogene in melanoma
17	*Akap8l*	3	4.4 - 11.8	A-kinase anchoring protein, recruits cAMP-dependent protein kinase (PKA) to chromatin
18	*Pdp1*	3	4.1 - 9.8	Pyruvate dehydrogenase phosphatase 1, regulation of glucose metabolism
19	*Yes1*	3	5.4 - 9.7	Src family kinase, oncogene in several tumours
20	*Met*	3	4.1 - 8.9	Receptor tyrosine kinase, involved in hepatocellular and other cancers
21	*Ppm1g*	3	6.2 - 8.2	Dephosphorylates spliceosome substrates and histones H2A-H2B
22	*Blvrb*	3	5.3 - 8.0	Biliverdin reductase, also transcription factor, arrest of cell cycle
23	*Tnk1*	3	5.2 - 7.6	Downregulates Ras pathway (phosphorylation of Grb2), inhibition of NF-kB pathway
24	*Prkab2*	3	4.1 - 7.0	Subunit of AMP kinase, inhibits fatty acid synthesis and mTOR pathway
25	*Trpm7*	3	4.9 - 5.9	Ion channel and serine-threonine kinase
26	*Ppp3cc*	3	4.2 - 4.4	Regulatory subunit of calcineurin (phosphatase in T cell receptor signaling)

Secondary screens were performed with a total of approximately 15 shRNAs for each gene of interest. **a**, Results from secondary screen of T-cell dysfunction pool shRNA library. Genes for which at least three shRNAs showed ≥ fourfold enrichment in tumours are listed, along with a brief description of their function. **b**, Results from secondary screen of kinase and phosphatase shRNA libraries.